ORIGINAL ARTICLE

JBMR®

Assessment of Bone Fragility in Patients With Multiple Myeloma Using QCT-Based Finite Element Modeling

Graeme M Campbell,[1,2] Jaime A Peña,[1] Sarah Giravent,[1] Felix Thomsen,[3] Timo Damm,[1] Claus-C Glüer,[1] and Jan Borggrefe[1,4]

[1]Section Biomedical Imaging, Department of Radiology and Neurology, University Hospital Schleswig-Holstein, Kiel, Germany
[2]Institute of Biomechanics, Hamburg University of Technology, Hamburg, Germany
[3]National Scientific and Technical Research Council (CONICET), National University of the South, Bahía Blanca, Argentina
[4]Institut und Poliklinik für Diagnostische Radiologie, Uniklinik Köln, Köln, Germany

ABSTRACT

Multiple myeloma (MM) is a malignant plasma cell disease associated with severe bone destruction. Surgical intervention is often required to prevent vertebral body collapse and resulting neurological complications; however, its necessity is determined by measuring lesion size or number, without considering bone biomechanics. Finite element (FE) modeling, which simulates the physiological loading, may improve the prediction of fragility. To test this, we developed a quantitative computed tomography (QCT)-based FE model of the vertebra and applied it to a dataset of MM patients with and without prevalent fracture. FE models were generated from vertebral QCT scans of the T_{12} (T_{11} if T_{12} was fractured) of 104 MM patients, 45 with fracture and 59 without, using a low-dose scan protocol (1.5 mm slice thickness, 4.0 to 6.5 mSv effective dose). A calibration phantom enabled the conversion of the CT Hounsfield units to FE material properties. Compressive loading of the vertebral body was simulated and the stiffness, yield load, and work to yield determined. To compare the parameters between fracture and nonfracture groups, *t* tests were used, and standardized odds ratios (sOR, normalized to standard deviation) and 95% confidence intervals were calculated. FE parameters were compared to mineral and structural parameters using linear regression. Patients with fracture showed lower vertebral stiffness (–15.2%; $p = 0.010$; sOR = 1.73; 95% CI, 1.11 to 2.70), yield force (–21.5%; $p = 0.002$; sOR = 2.09; 95% CI, 1.27 to 3.43), and work to yield (–27.4%; $p = 0.001$; sOR = 2.28; 95% CI, 1.33 to 3.92) compared to nonfracture patients. All parameters correlated significantly with vBMD (stiffness: $R^2 = 0.57$, yield force: $R^2 = 0.59$, work to yield: $R^2 = 0.50$, $p < 0.001$), BV/TV (stiffness: $R^2 = 0.56$, yield force: $R^2 = 0.58$, work to yield: $R^2 = 0.49$, $p < 0.001$), and Tb.Sp (stiffness: $R^2 = 0.51$, yield force: $R^2 = 0.53$, work to yield: $R^2 = 0.45$, $p < 0.001$). FE modeling identified MM patients with compromised mechanical integrity of the vertebra. Higher sOR values were obtained for the biomechanical compared to structural or mineral measures, suggesting that FE modeling improves fragility assessment in these patients. © 2016 American Society for Bone and Mineral Research.

KEY WORDS: BONE QCT; PRIMARY TUMORS OF BONE AND CARTILAGE; BIOMECHANICS; RADIOLOGY

Introduction

Multiple myeloma (MM) is a malignant plasma cell disease of unknown cause, accounting for approximately 1% of all malignant disease cases and approximately 10% of hematologic malignancies.[1,2] MM is associated with bone destruction and high fracture rates primarily in the vertebra,[3,4] which leads to severe pain, loss of mobility, and neurological complications. This results from diffuse or osteolytic lesions that occur in approximately 80% of patients,[5] and contributes to increased morbidity and mortality, as well as reduced quality of life.[3,6–8] Assessment of bone fragility in MM patients is of particular importance in order to make a decision on whether to refer to surgical treatment, vertebroplasty, or radiotherapy.[9,10] This assessment is currently based on determining the number or size of focal lesions[10,11] or cortical erosion[12] from radiographs; however, these methods do not consider the biomechanical aspects of the vertebral body and therefore may not sufficiently identify those patients requiring intervention.

Computer simulations of loading on the vertebral body using finite element (FE) models based on quantitative computed tomography (QCT) scans enhances the assessment of bone fragility over measures of areal bone mineral density (aBMD) from dual-energy X-ray absorptiometry (DXA) and volumetric bone mineral density (vBMD) from QCT.[13–15] In these models, the vertebral body is divided into a large number of elements, each of which is assigned material properties based on the local vBMD value.[16] The compressive loading on the vertebral body is then simulated and the whole-bone stiffness and strength determined. Low-dose whole-body CT enables a comprehensive assessment of the entire spine and has recently been shown to provide superior detection of lesions compared to conventional

Received in original form April 25, 2016; revised form July 20, 2016; accepted July 21, 2016. Accepted manuscript online July 25, 2016.
Address correspondence to: Graeme Campbell, PhD, Institute of Biomechanics, Hamburg University of Technology, Denickestrasse 15, 21073 Hamburg, Germany. E-mail: graeme.campbell@tuhh.de

Journal of Bone and Mineral Research, Vol. 32, No. 1, January 2017, pp 151–156
DOI: 10.1002/jbmr.2924

X-ray in patients with MM.[17] Using a similar low-dose protocol, we have previously shown that the measurement of mineral (vBMD) and structural parameters such as bone volume fraction (BV/TV) and trabecular separation (Tb.Sp) with QCT permits the discrimination of vertebral fracture status.[18,19] By incorporating geometrical, structural, and mineral properties of the vertebral body, QCT-based FE models may provide a superior ability to identify patients at risk of skeletal complications and fracture; however, the degree to which these models can identify vertebrae with compromised biomechanics in patients with MM has not yet been studied.

Therefore, the objective of this cross-sectional study was to test the potential for FE models based on low-dose QCT scan protocols of the vertebra to distinguish between MM patients with and without prevalent fracture.

Patients and Methods

Study design and participants

QCT scans of 178 patients referred to the Department of Radiology, UKSH Campus Kiel, for non–contrast enhanced CT scans with the indication of staging for myeloma were used for this study. In a cross-sectional analysis, the first CT scan of each patient between January 2010 and January 2012 was examined. All patients with MM had received thalidomide treatment preceding the study. The study was approved by the local ethics commission (registration ID: D 430/12) and was designed to meet good clinical practice (GCP) criteria (http://www.ich.org/products/guidelines.html). Patients were excluded from the investigation if they had not permitted data use for study purpose at admission or if they met the following exclusion criteria: previous malignancy, known metabolic bone disorders, history of sprue, radiation of the spine, abnormal thyroid function, or other clinical studies. Vertebral compression fractures were diagnosed according to the Genant criteria.[20] All patients with a fracture of both T_{11} and T_{12} were excluded from the investigation. Fifty of 178 patients were excluded due to these criteria. A further 13 patients were excluded in the outlier analysis due to beam hardening artifacts and protocol errors and 11 patients were excluded due to diffuse osteolytic lesions of the entire spine that included T_{11} and T_{12}.

QCT scan protocol

All patients were scanned on the same Siemens Somatom Sensation 64 CT scanner (Siemens AG, Erlangen, Germany). Scans of T_{12} (or of T_{11} in the case that the T_{12} was fractured or showed macroscopic evidence of osteolytic lesions) were conducted with the preexisting CT protocol with 120 kVp, 100 mAs, and a 1.5-mm slice thickness resulting in a effective dose of approximately 4.0 to 6.5 mSv (International Commission on Radiological Protection [ICRP] Publication 103). The scan extent for the calculated effective dose was from top of the skull down to the knees. The InTable calibration phantom (Image Analysis Inc., Columbia, KY, USA) embedded in the CT mat underneath the patient was included in all CT scans thus permitting quantitative CT analyses. The CT data were reconstructed with the B70s reconstruction kernel in two different formats: (1) a regular resolution reconstruction used for vBMD calibration encompassing the entire cross-section of the patient and the calibration phantom underneath the patient and (2) a higher-resolution reconstruction (120 mm field of view [FOV], 512×512 pixels) limited to the vertebral body, which was used for vBMD and microstructural analyses, as well as for the development of the FE model. Longitudinal quality assurance to ensure stability of the scanner throughout the study was performed using a Mindways Type 3 QA- and calibration-phantom (Mindways, Austin, TX, USA). The in-house QCT software StructuralInsight (V.3.0)[21–23] was adapted to convert the Hounsfield unit value to the BMD value of each voxel (BMD_{VOX}) using the InTable calibration phantom. The endosteal and periosteal surfaces of the vertebral body, as well as the upper and lower endplates were defined using a semiautomatic bone segmentation procedure in StructuralInsight. The vertebral volume was calculated as the volume within the periosteal surface. The vBMD as well as the structural parameters of BV/TV and Tb.Sp were calculated and have been reported in a prior publication.[19] These values were used for comparison with the FE parameters that are outlined in the following section (FE modeling).

FE modeling

In order to simulate the loading on the vertebral bodies in the FE model, the vertebral CT images were aligned to the vertical axis in StructuralInsight. This was accomplished by computing best-fit planes from the voxels of the upper and lower endplates, and aligning the image to the average of these two planes. Following alignment, the meshes were generated using a custom-built program in Matlab (v2014a; Mathworks, Natick, MA, USA). The images were first scaled in plane to give an isotropic voxel size and then meshed with linear tetrahedral elements using the iso2mesh toolbox (http://iso2mesh.sourceforge.net) (Fig. 1). The number of elements in each model was on the order of 10,000 (14724 ± 6191) and the maximum volume of each element was restricted to 7 mm^3. The linear elements were converted to quadratic elements using custom Matlab scripts. In order to simulate the heterogeneity of the mechanics throughout the vertebral body, the material properties of each element were determined from the QCT data. This was accomplished by obtaining BMD_{VOX} from the Hounsfield unit value of each voxel using a linear regression of the calibration phantom reference values. The BMD of each element (BMD_{EL}) was then taken as the average BMD_{VOX} of all voxels whose centroids lay within the element. The elemental stiffness and yield stress were then derived from these values according to Keyak[16] to create elastic-perfectly plastic material behavior.

The loading conditions of a standard compressive mechanical test on the vertebral bodies were then simulated (Fig. 1). A layer of poly(methyl methacrylate) (PMMA) with a thickness of 5 mm was assumed on both the proximal and distal surfaces. The nodes on the distal surface of the vertebral body were fixed while those on the proximal surface were displaced by 1 mm in compression using a 0.01-mm step size. The input files were solved using Calculix (version 2.8; http://www.calculix.de). The total reaction force at each loading step was calculated to generate a force-displacement curve of the simulation. From this curve, the stiffness, yield load, and work to yield were determined for each vertebral body using custom Matlab scripts.

Statistical analysis

Statistical analyses were performed using JMP 9.0 software (SAS Institute, Cary, NC, USA). Descriptive statistics for normally distributed variables are presented as mean $\pm$ standard deviation unless noted otherwise. Student's *t* tests were performed for assessing differences between fracture and nonfracture groups for each parameter. Age-adjusted standardized odds ratios (sOR)

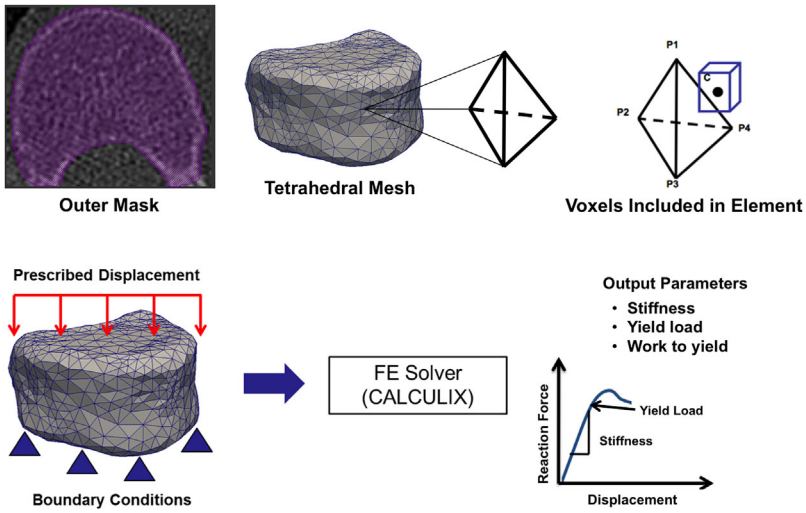

Fig. 1. Finite element analysis procedure. (Top) The vertebral body is isolated from the CT images using a semiautomated contouring procedure in StructuralInsight. The resulting segmented mask is converted into a mesh consisting of quadratic tetrahedral elements using iso2mesh and custom Matlab scripts. The elemental stiffness, yield stress and yield strain are then determined according to the vBMD of the voxels within the element. (Bottom) Axial compression was applied to the upper nodes while the bottom nodes were fixed in place. The models were solved using Calculix and the total reaction force calculated at each step and plotted to create a force-displacement curve. The stiffness, yield force, and work to yield were determined from the curve.

per standard deviation of the distribution of the patients without fractures and their 95% confidence intervals (CIs) were calculated from logistic regression analysis. Correlations between FE and QCT parameters were determined using linear regression.

Results

The patient group meeting all of the study criteria consisted of 104 patients, 60 men and 44 women, aged 31 to 89 years (mean 63.3 ± 11 years). This also included patients with monoclonal gammopathy of undetermined significance (MGUS)[24] ($n = 15$) or MM without disseminated bone disease (Durie and Salmon Grade [S&D], $n = 12$). The majority of patients showed advanced MM to S&D grade 2 ($n = 9$) or grade 3 ($n = 68$). Twenty-three of the 60 men (38%) and 22 of the 44 women (50%) showed prevalent vertebral fracture of the T_{11} or T_{12} and were included in the fracture group. The remaining patients were included in the nonfracture group.

All FE parameters were significantly reduced in the prevalent fracture group compared to the nonfracture group as shown in Fig. 2 (stiffness: –15.2%, $p = 0.010$; yield force: –21.5%, $p = 0.002$; work to yield: –27.4%, $p = 0.001$). Significant sORs were also observed for all FE parameters (Table 1) with work to yield showing the highest sOR of 2.28 (95% CI, 1.33 to 3.92) followed by yield force with an sOR of 2.09 (95% CI, 1.27 to 3.43) and stiffness with an sOR of 1.73 (95% CI, 1.11 to 2.70). When analyzing separately for men and women, significantly lower stiffness (–18.7%, $p = 0.017$), yield force (–26.5%, $p = 0.003$), and work to yield (–34.3%, $p = 0.005$) were observed in the men with prevalent fracture. No group differences were observed in the women; however, the mechanical measures all trended toward lower values in the fracture cohort. Similarly, significant sORs for stiffness (2.06; 95% CI, 1.11 to 3.83), yield force (2.87; 95% CI, 1.33 to 6.19), and work to yield (4.11; 95% CI, 1.55 to 10.91) were observed in the men, but none was observed in the women. In both the combined and sex-specific analysis, yield force and work to yield demonstrated a higher sOR compared to

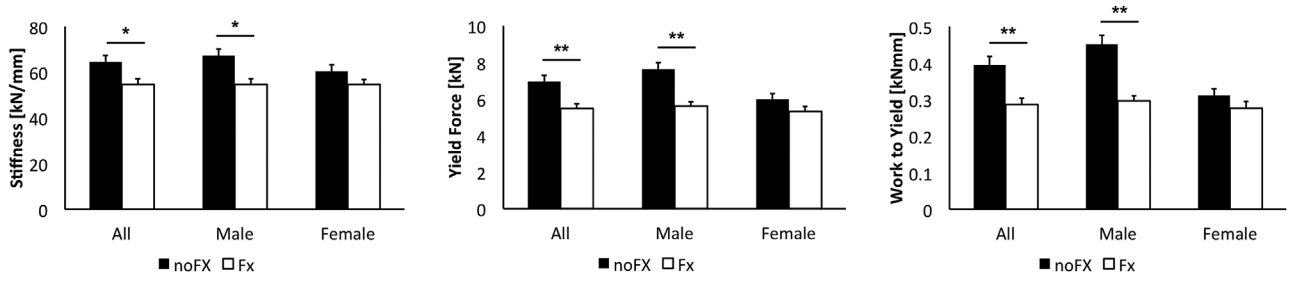

Fig. 2. Group means for apparent level stiffness, yield force, and work to yield in the noFx and Fx group. Group differences were determined for the entire cohort as well as separately for men and women. $^{*}p < 0.05$, $^{**}p < 0.01$ for group differences between Fx and noFx patients. Fx = fracture; noFx = nonfracture.

Table 1. Age-Adjusted Odds Ratios (±95% CIs) Normalized to Standard Deviation for the Entire Cohort, Women Only, and Men Only

	All patients	Women	Men
Stiffness	**1.73 (1.11–2.70)**	1.23 (0.63–2.44)	**2.06 (1.11–3.83)**
Yield force	**2.09 (1.27–3.43)**	1.26 (0.64–2.48)	**2.87 (1.33–6.19)**
Work to yield	**2.28 (1.33–3.92)**	1.19 (0.63–2.27)	**4.11 (1.55–10.91)**
Trabecular vBMD[a]	**1.6 (1.1–2.5)**	1.4 (0.8–2.6)	**2.1 (1.1–3.9)**
Cortical vBMD[a]	1.4 (0.9–2.1)	1.8 (0.9–3.2)	1.1 (0.7–1.9)
BV/TV[a]	**1.7 (1.1–2.5)**	1.1 (0.6–2.4)	**2.3 (1.2–4.2)**
Tb.Sp[a]	**2.4 (1.5–3.9)**	**2.1 (1.1–4.1)**	**3.0 (1.5–5.6)**

Bold values are significant ($p < 0.05$).
[a]Results presented previously.[19]

trabecular vBMD, cortical vBMD and BV/TV (Table 1). In the combined and female cohorts, Tb.Sp provided the highest sOR, whereas in the males, work to yield had the highest sOR.

Comparing the male and female cohorts, men showed higher yield force and work to yield compared to the women in the combined fracture and nonfracture dataset (yield force, men: 6.90 ± 2.77 kN, women: 5.67 ± 2.13 kN, $p = 0.016$; work to yield, men: 392.6 ± 191.9 MPa, women: 294.0 ± 138.4 MPa, $p = 0.005$) as well as in the nonfracture group (yield force, men: 7.77 ± 2.97 kN, women: 5.99 ± 2.33 kN, $p = 0.019$; work to yield, men: 457.8 ± 210.7 MPa, women: 311.0 ± 140.6 MPa, $p = 0.005$). In the fracture-only cohort, the yield force and work to yield were not significantly different between men and women. Men showed significantly larger vertebral volume compared to women in the combined (men: $29.7 \pm 5.26\ cm^3$, women: $23.4 \pm 4.01\ cm^3$), fracture-only (men: $28.7 \pm 5.18\ cm^3$, women: $23.8 \pm 3.94\ cm^3$), and nonfracture (men: $30.4 \pm 5.27\ cm^3$, women: $23.0 \pm 4.13\ cm^3$) cohorts.

The results of the linear regression analysis between FE parameters and vBMD, BV/TV, and Tb.Sp are shown in Fig. 3. Stiffness, yield force, and work to yield all correlated positively with vBMD (stiffness: $R^2 = 0.57$, yield force: $R^2 = 0.59$, work to yield: $R^2 = 0.50$, $p < 0.001$) and BV/TV (stiffness: $R^2 = 0.56$, yield force: $R^2 = 0.58$, work to yield: $R^2 = 0.49$, $p < 0.001$), whereas the FE parameters all correlated negatively with Tb.Sp (stiffness: $R^2 = 0.51$, yield force: $R^2 = 0.53$, work to yield: $R^2 = 0.45$, $p < 0.001$). Considering men and women separately, the association between all FE parameters and vBMD remained significant, where consistently higher correlation coefficients were observed in the men (data not shown).

Discussion

The goal of this study was to test the feasibility of QCT-based FE models of the vertebra to assess bone fragility in patients with

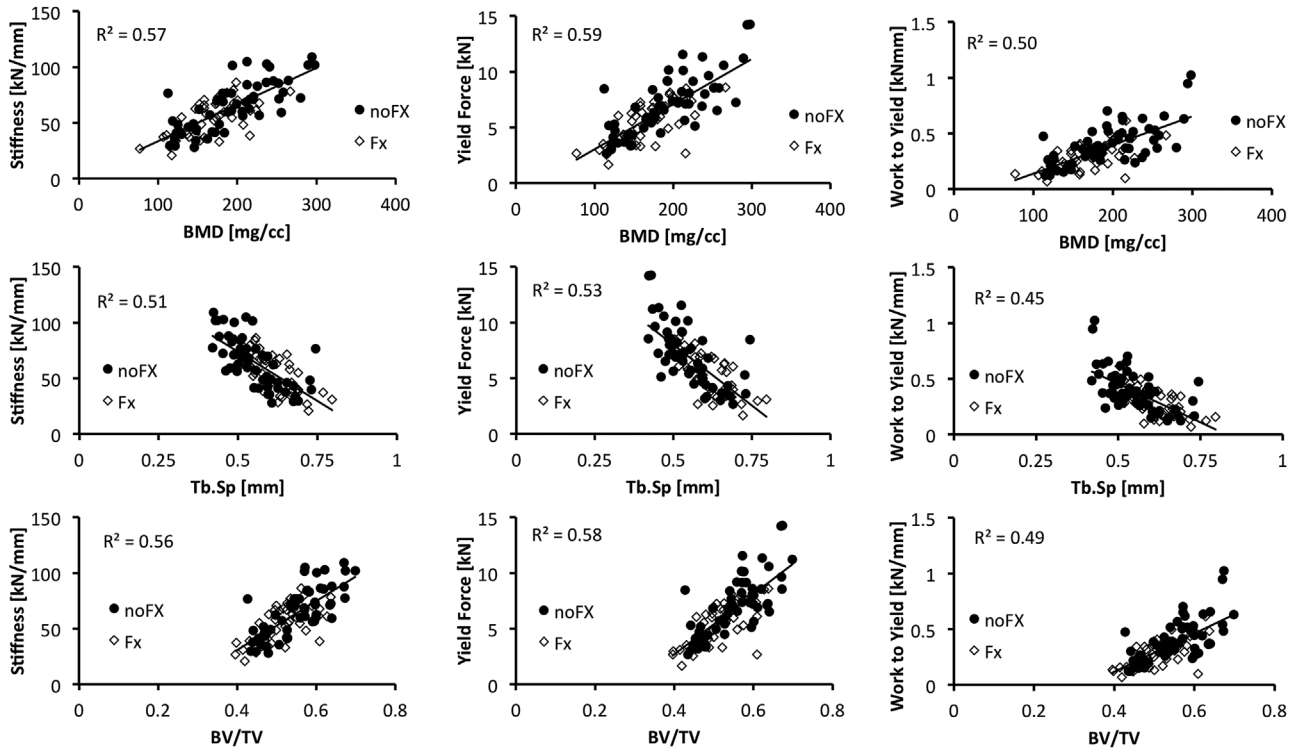

Fig. 3. Linear regression analysis of FE versus mineral and structural parameters. Fracture patients are depicted in open diamonds and nonfracture patients in filled circles.

MM. We show that the biomechanical parameters produced by the models distinguished between patients with and without prevalent fracture, suggesting that these methods may improve the ability to identify patients that require surgery to restore mechanical stability of the vertebra.

The analysis of sORs indicate that those patients with FE stiffness or strength parameters one standard deviation below the mean of the nonfracture groups are up to four times as likely to experience a vertebral fracture. Because the models were based on vertebrae without visible fracture, this suggests that osteolytic destruction takes place before possible observation by the radiologist, but can be detected earlier using FE methods. Localized destruction of the cortical and trabecular network from metastatic lesions can increase fragility with minimal effect on overall mineral and structural parameters,[18] which likely explains the higher sORs observed with biomechanical parameters compared to vBMD and BV/TV. The yield parameters (yield force and work to yield) consistently resulted in the highest sORs compared to stiffness. The stiffness represents the mechanical competence of the vertebral body under a relatively low state of loading, where no permanent deformation or local failure has occurred. In contrast, the yield parameters provide a more detailed assessment of how the structure deforms under larger loads and when local failure does occur. The results presented here suggest that not only are the structural and mineral properties in the fracture cohort inferior, but the ability to resist local failure as well, which results in earlier fracture of the bone.

In general, the biomechanical parameters all correlated well with the mineral and structural parameters ($0.45 < R^2 < 0.59$). Interestingly, the lowest correlations were observed with work to yield, the parameter with the highest sOR. This suggests that this parameter incorporates some independent information that is not provided from the vBMD or mean bone structure that is critical for mechanical integrity. This may include localized bone destruction resulting from osteolytic activity. It is important to note that the structural parameters presented here and in the previous work (BV/TV, Tb.Sp) are limited by the spatial resolution of the system. Both of these parameters are used extensively in micro–computed tomography (μCT) imaging where a voxel size of approximately 5 to 20 μm enables the accurate depiction of individual trabecular elements. However, with the much lower spatial resolution of clinical CT, the trabecular structure cannot be depicted in detail and consequently, these measurements will have larger errors and reduced reliability.

The predictive ability of FE analysis may be influenced by sex, because the models were unable to distinguish between fracture and nonfracture groups in the female cohort. This is in line with our previous work showing a lack of discriminatory power of vBMD and BV/TV in female patients. The vertebrae of the males were found to be stronger than those of the females in the nonfracture group, but have similar strength to the females in the fracture group. This suggests that within the nonfracture cohort, more women may be at risk of fracture than the men; however, future work using prospective data is required in order to confirm whether this is the case, and whether these patients can be identified with FE models. On the other hand, a larger number of men than women were referred in this study, and this may also have contributed to the lack of significance when considering the sexes separately. Nevertheless, trends toward differences between fracture groups in the females were observed for FE stiffness ($p = 0.092$), suggesting that with some refinement or more patients, FE models may have better discriminatory power in the female demographic as well.

The predicted mechanical behaviors from the FE models presented here generally agree with previous reports from compressive tests of excised vertebrae; however, some differences can be observed. Yield and fracture loads ranging from 2 to 9 kN have been reported for the vertebral bodies of the thoracic and lumbar spine,[25–28] and our predicted yield loads of 5 kN and 7 kN (fracture and nonfracture group, respectively) fall within this range. On the other hand, the vertebral stiffness values from Dall'Ara and colleagues[27] range from 17 and 54 kN/mm, which are lower than the values predicted in our model (55 kN/mm and 65 kN/mm in the fracture and nonfracture group, respectively). However, in this same study Dall'Ara and colleagues[27] also observed an overestimation of stiffness in their models, which gave values in the range of 27 kN to 70 kN, and our predicted values do lie within this range. This suggests that a general discrepancy between the FE models and the real loading conditions remains. Methods to refine the FE models in order to improve the bone fragility prediction could include improvement of the cortical shell representation. The vertebral bodies consist of a dense, thin cortical shell ($<$0.5 mm) that surrounds a less dense trabecular network. Because the elements of our model are larger than the CT voxel size, the surface elements will derive their material properties from a mean of both cortical and trabecular voxels. The resulting modulus of these elements is therefore lower than pure cortical bone but higher than pure trabecular bone. This is compounded by the fact that the voxels themselves are larger than the cortical thickness, resulting in partial volume averaging. Improvement of the cortical shell representation and model accuracy may be achieved through the use of specialized thin-shell elements to represent the cortex,[26,28,29] combined with accurate local thickness measurements obtained through the application of de-blurring techniques.[30] In addition, recent advancements in CT technology could improve bone fragility assessment. The use of dual-source CT, iterative reconstruction methods,[31] or image upsampling,[32] either during the reconstruction process or post hoc, may enable better distinction of the cortical shell and endplates. Furthermore, the FE models developed here assumed isotropic material properties; ie, the material properties were set to be identical in all directions. However, recent work has shown that the degree of anisotropy in the trabecular bone of the vertebra is significantly increased in female patients with MM,[33] and that inclusion of this parameter improves the prediction of strength in osteoporotic bone.[34] The incorporation of these microstructural attributes of the vertebral body to future FE models may therefore improve the assessment of bone fragility in MM patients without the need for higher-dose scan protocols.

This study shows that QCT-based FE models obtained from low-dose scan protocols, which simulate the biomechanical loading conditions on the vertebra, provide a superior assessment of bone fragility in patients with MM compared to mineral and structural measures. This method has the potential to identify patients at risk of fracture and may offer a superior alternative for radiologists to make decisions on treatment protocols. Future work will include the refinement of the FE models to more accurately represent the vertebral bone structure, as well as the application to prospective data to assess the ability of these methods to predict vertebral fracture.

Disclosures

All authors state that they have no conflicts of interest.

Acknowledgments

This work was supported by grants from the Deutsche Forschungsgemeinschaft (DFG) through the Forschergruppe 1586 SKELMET (CCG), by the research grant from the state of Schleswig-Holstein and the European Union ERDF-European Regional Development Fund (MOIN CC, Zukunftsprogramm Wirtschaft), and by the German Society for Osteology (DGO) (GC).

Authors' roles: Study design: GMC, JB, and CCG. Study conduct: GMC, SG, FT, JB, and CCG. Data collection: GMC, SG JB, and CCG. Data analysis: GMC, JP, and TD. Data interpretation: GMC, SG, JP, TD, JB, and CCG. Drafting manuscript: GMC. Revising manuscript content: GMC, SG, JP, FT, TD, JB, and CCG. Approval of final version of manuscript: GMC, SG, JP, FT, TD, JB, and CCG. GMC takes responsibility for the integrity of the data analysis.

References

1. Angtuaco EJ, Fassas AB, Walker R, Sethi R, Barlogie B. Multiple myeloma: clinical review and diagnostic imaging. Radiology. 2004;231(1):11–23.
2. Raab MS, Podar K, Breitkreutz I, Richardson PG, Anderson KC. Multiple myeloma. Lancet. 2009;374(9686):324–39.
3. Melton LJ 3rd, Kyle RA, Achenbach SJ, Oberg AL, Rajkumar SV. Fracture risk with multiple myeloma: a population-based study. J Bone Miner Res. 2005;20(3):487–93.
4. Lecouvet FE, Vande Berg BC, Michaux L, Jamart J, Maldague BE, Malghem J. Development of vertebral fractures in patients with multiple myeloma: does MRI enable recognition of vertebrae that will collapse? J Comput Assist Tomogr. 1998;22(3):430–6.
5. Bartl R, Fateh-Moghadam A. [The diagnosis of multiple myeloma]. Onkologie. 1986;9(4):183–8, 190–5.
6. Melton LJ 3rd, Rajkumar SV, Khosla S, Achenbach SJ, Oberg AL, Kyle RA. Fracture risk in monoclonal gammopathy of undetermined significance. J Bone Miner Res. 2004;19(1):25–30.
7. Vogel MN, Weisel K, Maksimovic O, et al. Pathologic fractures in patients with multiple myeloma undergoing bisphosphonate therapy: incidence and correlation with course of disease. AJR Am J Roentgenol. 2009;193(3):656–61.
8. Kyle RA, Gertz MA, Witzig TE, et al. Review of 1027 patients with newly diagnosed multiple myeloma. Mayo Clin Proc. 2003;78(1):21–33.
9. Winterbottom AP, Shaw AS. Imaging patients with myeloma. Clin Radiol. 2009;64(1):1–11.
10. Durie BG, Salmon SE. A clinical staging system for multiple myeloma. Correlation of measured myeloma cell mass with presenting clinical features, response to treatment, and survival. Cancer. 1975;36(3):842–54.
11. Baur-Melnyk A, Reiser M. [Staging of multiple myeloma with MRI: comparison to MSCT and conventional radiography]. Radiologe. 2004;44(9):874–81.
12. Delorme S, Baur-Melnyk A. Imaging in multiple myeloma. Eur J Radiol. 2009;70(3):401–8.
13. Kalpakcioglu BB, Engelke K, Genant HK. Advanced imaging assessment of bone fragility in glucocorticoid-induced osteoporosis. Bone. 2011;48(6):1221–31.
14. Crawford RP, Cann CE, Keaveny TM. Finite element models predict in vitro vertebral body compressive strength better than quantitative computed tomography. Bone. 2003;33(4):744–50.
15. Wang X, Sanyal A, Cawthon PM, et al. Prediction of new clinical vertebral fractures in elderly men using finite element analysis of CT scans. J Bone Miner Res. 2012;27(4):808–16.
16. Keyak JH. Improved prediction of proximal femoral fracture load using nonlinear finite element models. Med Eng Phys. 2001;23(3):165–73.
17. Horger M, Claussen CD, Bross-Bach U, et al. Whole-body low-dose multidetector row-CT in the diagnosis of multiple myeloma: an alternative to conventional radiography. Eur J Radiol. 2005;54(2):289–97.
18. Borggrefe J, Giravent S, Campbell G, et al. Association of osteolytic lesions, bone mineral loss and trabecular sclerosis with prevalent vertebral fractures in patients with multiple myeloma. Eur J Radiol. 2015 Nov; 84(11):2269–74.
19. Borggrefe J, Giravent S, Thomsen F, et al. Association of QCT bone mineral density and bone structure with vertebral fractures in patients with multiple myeloma. J Bone Miner Res. 2015;30(7):1329–37.
20. Genant HK, Wu CY, van Kuijk C, Nevitt MC. Vertebral fracture assessment using a semiquantitative technique. J Bone Miner Res. 1993;8(9):1137–48.
21. Graeff C, Campbell GM, Pena J, et al. Administration of romosozumab improves vertebral trabecular and cortical bone as assessed with quantitative computed tomography and finite element analysis. Bone. 2015;81:364–9.
22. Graeff C, Chevalier Y, Charlebois M, et al. Improvements in vertebral body strength under teriparatide treatment assessed in vivo by finite element analysis: results from the EUROFORS study. J Bone Miner Res. 2009;24(10):1672–80.
23. Graeff C, Marin F, Petto H, et al. High resolution quantitative computed tomography-based assessment of trabecular microstructure and strength estimates by finite-element analysis of the spine, but not DXA, reflects vertebral fracture status in men with glucocorticoid-induced osteoporosis. Bone. 2013;52(2):568–77.
24. International Myeloma Working Group. Criteria for the classification of monoclonal gammopathies, multiple myeloma and related disorders: a report of the International Myeloma Working Group. Br J Haematol. 2003;121(5):749–57.
25. Fields AJ, Lee GL, Liu XS, Jekir MG, Guo XE, Keaveny TM. Influence of vertical trabeculae on the compressive strength of the human vertebra. J Bone Miner Res. 2011;26(2):263–9.
26. Liebschner MA, Kopperdahl DL, Rosenberg WS, Keaveny TM. Finite element modeling of the human thoracolumbar spine. Spine. 2003;28(6):559–65.
27. Dall'Ara E, Pahr D, Varga P, Kainberger F, Zysset P. QCT-based finite element models predict human vertebral strength in vitro significantly better than simulated DEXA. Osteoporos Int. 2012;23(2):563–72.
28. Imai K, Ohnishi I, Bessho M, Nakamura K. Nonlinear finite element model predicts vertebral bone strength and fracture site. Spine. 2006;31(16):1789–94.
29. Chevalier Y, Pahr D, Zysset PK. The role of cortical shell and trabecular fabric in finite element analysis of the human vertebral body. J Biomech Eng. 2009;131(11):111003.
30. Treece GM, Gee AH, Mayhew PM, Poole KE. High resolution cortical bone thickness measurement from clinical CT data. Med Image Anal. 2010;14(3):276–90.
31. Geyer LL, Schoepf UJ, Meinel FG, et al. State of the art: iterative CT reconstruction techniques. Radiology. 2015;276(2):339–57.
32. Hwang SN, Wehrli FW. Subvoxel processing: a method for reducing partial volume blurring with application to in vivo MR images of trabecular bone. Magn Reson Med. 2002;47(5):948–57.
33. Takasu M, Tani C, Ishikawa M, et al. Multiple myeloma: microstructural analysis of lumbar trabecular bones in patients without visible bone lesions—preliminary results. Radiology. 2011;260(2):472–9.
34. Fields AJ, Eswaran SK, Jekir MG, Keaveny TM. Role of trabecular microarchitecture in whole-vertebral body biomechanical behavior. J Bone Miner Res 2009;24(9):1523–30.